Reconfigurable SoC-Based Smart Sensor for Wavelet and Wavelet Packet Analysis

Rene J. Romero-Troncoso, *Member, IEEE*, Marcos Pena-Anaya, Eduardo Cabal-Yepez, *Member, IEEE*, Arturo Garcia-Perez, *Member, IEEE*, and Roque A. Osornio-Rios, *Member, IEEE*

***Abstract*—Modern monitoring systems require high-performance instrumentation, low-cost primary sensors, online signal processing, portability, and versatility. Smart sensor utilization is an approach to comply with these features. From an industrial point of view, voltage, electric current, and vibrations are signals commonly analyzed during system monitoring, and wavelet and wavelet packet transforms are popular techniques for extracting time-frequency information from these signals. Here, a system-on-chip-based smart sensor with reconfigurable architecture is proposed for time-frequency analysis applying either wavelet or wavelet packet transform. The proposed smart sensor uses a proprietary hardware processing unit and a custom embedded microprocessor. It can connect to different primary sensors without additional instrumentation and shows obtained results in a 2-D or 3-D view on a video graphics array screen or liquid crystal display. Obtained results from three different study cases demonstrate that the proposed smart sensor is able to show online and in real-time the frequency evolution effects in time-varying signals.**

***Index Terms*—Embedded microprocessor, reconfigurable architecture, smart sensor, system-on-chip (SoC), wavelet transform (WT).**

I. Introduction

NOWADAYS, monitoring systems face demanding tasks that require high-performance instrumentation, low-cost primary sensors, and characteristics of online signal processing. Portability and versatility are not easily met by commercially available monitoring equipment. In industry, different parameters such as voltage, electric current, and vibrations are sensed. They are analyzed through different signal processing techniques to observe dynamic characteristics of analyzed systems. Usually, signals are acquired by primary sensors in the form of independent instruments, whereas signal processing is carried out offline through complex techniques such as time-frequency analyses. The whole monitoring process represents extra cost for users because of the customization in the instrumentation of commercially available equipment. The utilization of smart sensors is a promising approach to increase performance and overcome costs in monitoring systems. They use standard off-the-shelf sensors and add signal processing, communication, and integration capabilities in their functionality [1], [2].

Many monitoring systems based on smart sensors have been proposed in past years. For instance, in [3], a smart sensing system for flavor analysis of liquids is proposed based on acoustic wave sensors and sensors for liquid and gaseous phase analysis. In [4], an intelligent sensor for detecting hydrogen leaks and nitrogen oxide concentration in automotive applications is developed. A smart sensor for medium-voltage dc power grid protection is proposed in [5] via current and voltage transformers. In [6], a smart sensor for real-time high-resolution frequency estimation in power systems is proposed through an off-the-shelf current clamp sensor. In [7], a smart sensor system for machine fault diagnosis is developed by acquiring vibration, current, and flux signals from induction motors. From here, it is clear that today monitoring requires the sampling and analysis of several signals through different primary sensors and signal processing techniques to carry out reliable system monitoring; for this reason, some works focus on communicating different sensors in a single process. For instance, in [8], a sensor network connected through a universal serial bus (USB)-to-Ethernet gateway for industrial applications is proposed. A platform to interconnect independent smart sensors used for monitoring electric current, vibration, and position in a machining process is proposed in [9]. From an industrial point of view, voltage, electric current, and vibrations are common signals analyzed during system monitoring [5]–[9]; however, used smart sensors can be considered as application specific since they just process the particular signal acquired by their primary sensor and have to communicate through additional instrumentation and equipment, which increases the cost of system monitoring.

As stated above, a smart sensor includes signal processing, communication, and integration capabilities in its functionality. These features are met by a system-on-chip (SoC) design [10], [11]. Regarding signal processing, two of the most popular techniques are wavelet transform (WT) and wavelet packet transform (WPT). These techniques are able to extract time-frequency information from nonstationary signals. For instance, a wavelet-based approach to improve accuracy of quantized acoustoelectric current is proposed in [12]. In [13], wavelet analysis of vibration signals is used for determining system frequencies in mechanical systems. In [14], induction motor faults are detected by computing wavelet coefficients of induction motor startup current. On the other hand, in [15] and [16],

Manuscript received October 22, 2011; revised December 18, 2011; accepted January 10, 2012. Date of publication April 3, 2012; date of current version August 10, 2012. This work was supported in part by the National Council on Science and Technology (CONACYT), Mexico, under Scholarship 226882. The Associate Editor coordinating the review process for this paper was Dr. Kurt Barbe.

R. J. Romero-Troncoso, M. Pena-Anaya, E. Cabal-Yepez, and A. Garcia-Perez are with the Division de Ingenierias, Universidad de Guanajuato, 36700 Salamanca, Gto., Mexico (email: troncoso@hspdigital.org; mpena@hspdigital.org; ecabal@hspdigital.org; agarcia@hspdigital.org).

R. A. Osornio-Rios is with the Facultad de Ingenieria, Universidad Autónoma de Querétaro, 76807 San Juan del Rio, Qro., Mexico (e-mail: raosornio@hspdigital.org).

Color versions of one or more of the figures in this paper are available online at http://ieeexplore.ieee.org.

Digital Object Identifier 10.1109/TIM.2012.2190340

methods for induction motor condition monitoring through wavelet packet decomposition of electric current supply are presented. In [17], a diagnosis method applied to a polymer electrolyte fuel cell was introduced. This method analyzes the stack voltage signal through wavelet packed coefficients. From the formerly stated, it would be desirable to count with a reconfigurable smart sensor able to inspect different kinds of signal, such as voltage, electric current, and vibrations, among others, through common signal processing techniques such as WT and WPT. The smart sensor should be able to carry out complete system monitoring by just connecting it to each corresponding primary sensor rather than having costly monitoring systems with several independent sensors and processing units connected through a network.

The contribution of this work is a smart sensor integrated as a low-cost SoC. The proposed smart sensor is based on a reconfigurable hardware processing unit and a custom embedded processor implemented into a field-programmable gate array (FPGA). It can connect to different primary sensors to increase performance capabilities that allow the smart sensor to apply either WT or WPT analysis on the acquired signal, with different parameters (e.g., mother wavelet and decomposition level). Obtained results can be presented to the user in a 2-D or 3-D view with different perspectives. The proposed smart sensor permits modification or redefinition of the implemented algorithm without changing the hardware itself. It extracts relevant time-frequency information from different sampled signals such as voltage, electric current, and vibrations, among others, to carry out complete system monitoring. To verify the performance of the proposed smart sensor, three different signals from distinct study cases are acquired and WT or WPT is analyzed: voltage supply to an induction motor through a variable speed drive (VSD), electric current supply to an induction motor with broken rotor bars, and vibration signals from industrial robot links. Obtained results validate the usefulness of the proposed smart sensor to carry out time-frequency analysis during system monitoring.

II. Theoretical Background

WT and WPT are used for extracting time-frequency information from time-dependent signals. They are capable to give frequency decomposition of a signal through time by isolating its frequency evolution.

A. WT

Continuous WT is defined through the wavelet coefficients (WC) produced by the convolution of a signal $x(t)$ with a mother wavelet function $\psi(t)$ [18]. The transformation process gives a timescale decomposition of the original signal. The concept of scale is related to the concept of frequency and corresponds to a timescale a of function $\psi(t)$. The process also involves shifting b of the scaled mother wavelet function. This way, the transformation process can be described by

$$WC(a,b) = \frac{1}{\sqrt{|a|}} \int_{-\infty}^{\infty} x(t)\overline{\psi\left(\frac{t-b}{a}\right)}dt. \tag{1}$$

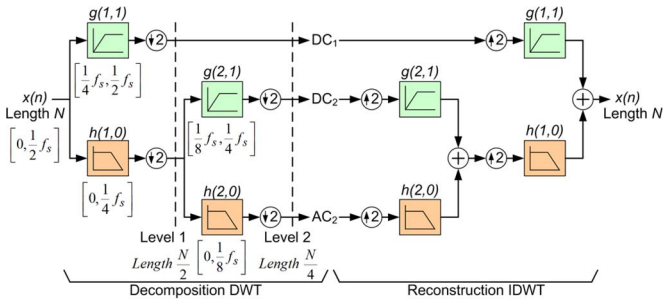

Fig. 1. Mallat algorithm for wavelet decomposition and reconstruction of discrete signals.

Discrete WT (DWT) has shown its value in analyzing nonstationary signals [12]–[14]. It is computed using a set of discrete-time low- and high-pass filters $h(i,j)$ and $g(i,j)$, respectively, followed by a signal downsampling operation for each decomposition level; this method is known as Mallat algorithm [19]. Indices i and j represent decomposition level and transformation-node number, respectively, as depicted in Fig. 1. According to this algorithm, the original discrete signal $x(n)$ is decomposed into its low- and high-frequency components named approximation (AC_i) and detail (DC_i), respectively, at level i. Decomposition is successively applied to AC_i in order to obtain subsequent low- and high-frequency bands down to the desired level L. The low- and high-frequency bands are given by (2) and (3), respectively, with f_s corresponding to the sampling frequency

$$AC_i \Rightarrow \left[0, \frac{f_s}{2^{i+1}}\right] \tag{2}$$

$$DC_i \Rightarrow \left[\frac{f_s}{2^{i+1}}, \frac{f_s}{2^i}\right]. \tag{3}$$

Once the discrete input signal $x(n)$ has been decomposed into L desired levels, signal reconstruction is done by applying the decomposition process in an inverse way. This time, each reconstruction level is followed by a signal upsampling operation. This is known as the inverse DWT (IDWT), as shown in Fig. 1.

B. WPT

Discrete WPT (DWPT) decomposes approximation and detail coefficients into their low- and high-frequency bands [20], which is different from DWT where just approximation coefficients are decomposed. The decomposition coefficients $S_{i,j}$ for each wavelet packet node $h(i,j)$ and $g(i,j)$ are obtained through the inner products of $x(n)$ with the corresponding wavelets, as depicted in Fig. 2. Signal reconstruction, known as the inverse DWPT (IDWPT), is carried out by applying the decomposition process in an inverse way.

III. Smart Sensor Implementation

A smart sensor provides signal processing and communication capabilities to the primary sensor. Characteristics such as portability and integration are included by implementing the

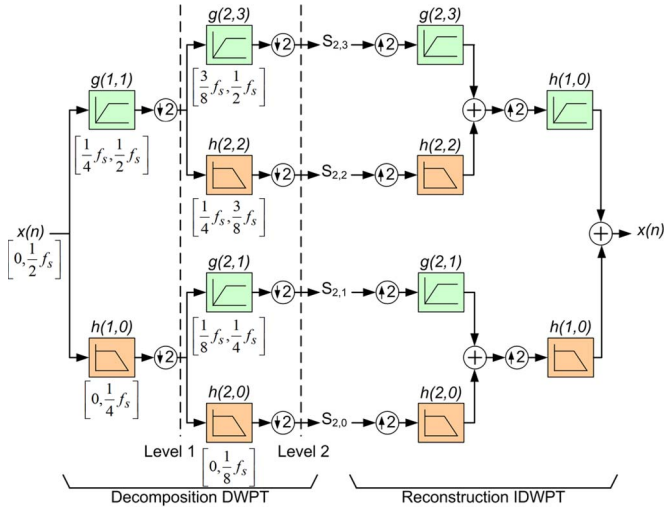

Fig. 2. Wavelet packet decomposition and reconstruction of discrete signals.

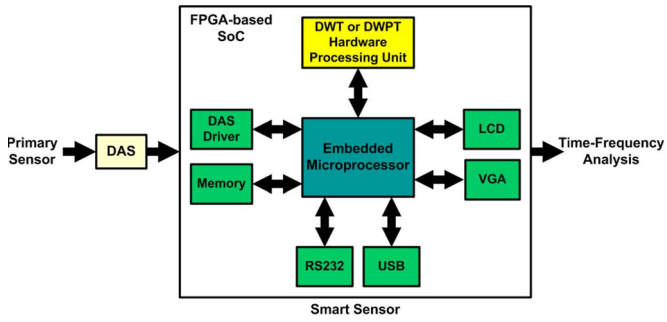

Fig. 3. Block diagram of the proposed SoC-based smart sensor.

smart sensor as a SoC. Fig. 3 depicts the block diagram of the proposed smart sensor realized into an FPGA-based SoC. All its components are developed in a very high-speed integrated-circuit hardware description language (VHDL) as proprietary cores. During time-frequency analysis for system monitoring, the signal is acquired and conditioned in the data acquisition system (DAS). The embedded microprocessor is in charge of information exchange, including signal acquisition through the DAS driver. A hardware processing unit is used for real-time computation of DWT or DWPT. Memory is required for temporal storage of information, and interfaces such as liquid crystal display (LCD), video graphics array (VGA), USB, and RS232 are used for displaying results to users or transferring information to a PC. Other interfaces for information transference can be easily incorporated into the smart sensor by developing the hardware description of their corresponding drivers.

A. Embedded Microprocessor

The embedded microprocessor in the proposed smart sensor is a proprietary 8-bit Harvard-architecture microprocessor implemented as a reduced instruction set computer. Different from previous approaches intended to improve some features in commercially available general-purpose microprocessors [21], the proprietary embedded microprocessor is customized for register transference and interrupt management to speed up program execution and reduce power consumption. Its main task is

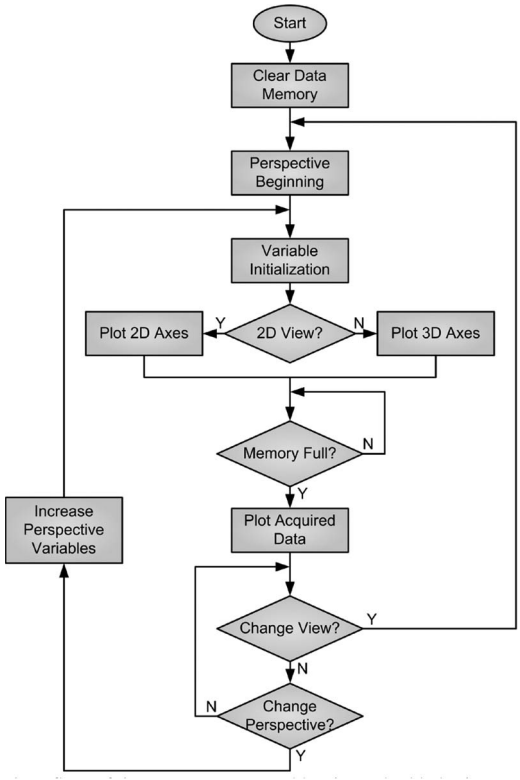

Fig. 4. Chart flow of the program executed by the embedded microprocessor.

to coordinate information exchange among components of the smart sensor. It works as an arbiter for information management from or to the user, which allows selecting different views (2-D or 3-D) and perspectives during the presentation and/or transmission of obtained results through different interfaces. Fig. 4 depicts the chart flow of the program executed by the microprocessor to plot obtained time-frequency results with different views and perspectives.

B. DWT or DWPT Hardware Processing Unit

DWT and DWPT implementations are particular cases of the finite-impulse-response filter (4), where $x(n)$ and $y(n)$ are the input and output sequences, respectively; M is the filter order; and $b_i (i = 0, 1, \ldots, M)$ are filter coefficients. For this reason, DWT and DWPT implementations are based on a multiply-accumulate (MAC) unit

$$y(n) = \sum_{i=0}^{M} b_i x(n-i). \tag{4}$$

Depending on the applied analysis, the DWT or DWPT hardware processing unit may require just a decomposition (DWT or DWPT) module or decomposition and reconstruction (IDWT or IDWPT) modules. This can be defined by the user along with the desired decomposition levels and the applied mother wavelet function during the smart sensor configuration.

C. Decomposition (DWT or DWPT)

During decomposition, the corresponding DWT or DWPT coefficients are extracted from a ROM device and multiplied by

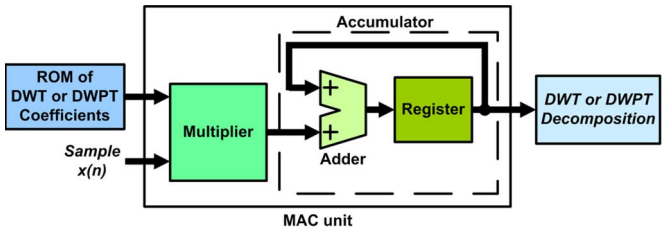

Fig. 5. Signal decomposition (DWT or DWPT) based on a MAC unit.

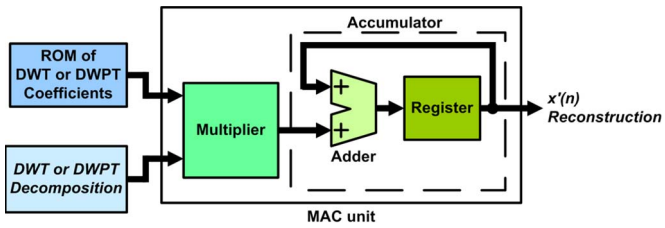

Fig. 6. Signal reconstruction (IDWT or IDWPT) based on a MAC unit.

the current signal sample $x(n)$; when a new sample is acquired, this operation is repeated and partial results are accumulated.

If reconstruction is required, partial decomposition coefficients are stored into on-chip block-RAM modules; otherwise, the proposed smart sensor can be configured to provide these coefficients at its output. The block diagram of the DWT or DWPT decomposition is depicted in Fig. 5.

D. Reconstruction (IDWT or IDWPT)

Signal reconstruction (IDWT or IDWPT) is carried out by multiplying DWT or DWPT coefficients by the corresponding wavelet components stored in on-chip block-RAM, which were obtained during signal decomposition. This procedure obtains a reconstructed sample $x'(n)$, as depicted in Fig. 6.

E. Smart Sensor Reconfigurability

A graphical user interface (GUI) is developed for configuring characteristics of the proposed smart sensor for time-frequency analysis. This application generates VHDL and assembly language code corresponding to the hardware in the smart sensor implementation and the program executed by the embedded microprocessor, respectively. Through this GUI tool shown in Fig. 7, the user does not have to write any code for reconfiguring the smart sensor.

During the smart sensor configuration, the user has to define parameters such as: 1) number of samples and sampling frequency; 2) maximum decomposition level and frequency bands of interest; 3) mother wavelet to be applied, which corresponds to any of the mother wavelet functions available in MATLAB; 4) used algorithm (DWT or DWPT; if one level is selected, DWPT is applied); 5) must be selected if reconstruction of the selected frequency bands is required; 6) by default, the obtained time-frequency analysis is shown on a VGA display, but an LCD can be selected; 7) generates hardware and software for the smart sensor implementation according to selected parameters; and 8) exits the application.

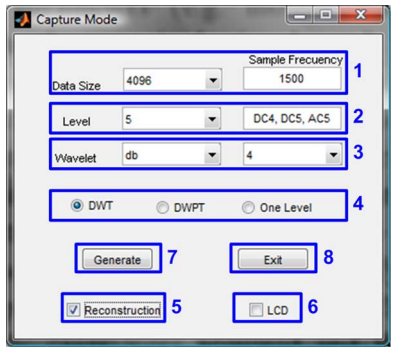

Fig. 7. GUI tool for hardware and software generation during the smart sensor implementation.

For communication purposes, the smart sensor is connected to a host system through a USB or RS232. Other interfaces such as local interconnect network [22], controller area network [23], and FlexRay and SpaceWire [24], among others, can be easily integrated into the smart sensor implementation by obtaining or developing the hardware description of their corresponding drivers and the assembly program executed in the embedded microprocessor to coordinate the information exchange.

IV. Experimentation and Results

This section describes experimental tests for verifying the performance of the proposed SoC-based smart sensor on computing DWT or DWPT. Different signals were acquired and time-frequency analyzed in three different study cases, namely, voltage supply to an induction motor through a VSD, current supply to an induction motor with broken rotor bars, and vibration signals from industrial robot links. Other signals can be monitored utilizing the proposed smart sensor by connecting the corresponding primary sensor and accordingly configuring the DAS during the smart sensor implementation. The analysis applied in the different study cases was heuristically chosen. Similarly, the decomposition levels and components (frequency bands) were selected so that the time-frequency evolution effects on the analyzed signal can be observed to a greater extent. This was possible because of the reconfigurability of the proposed smart sensor. For presentation purposes, hardware computed results were sent to a PC through an RS232 interface and plotted in MATLAB.

A. Experiment Setup for Voltage Signal Analysis

A VSD controls induction motor rotating speed from 0 to nominal frequency introducing time-varying harmonics into the voltage supply signal. Fig. 8 shows the experiment setup for carrying out time-frequency analysis of the voltage supply signal provided by a VSD. A three-phase 1-hp induction motor (model WEG 00136APE48T) with 2 poles and 28 bars is fed through a VSD (model WEG CFW-10). The motor rotational speed is controlled at 30, 45, and 60 Hz. The applied mechanical load is that of an ordinary alternator. The VSD output voltage signal is time-frequency analyzed utilizing the proposed smart sensor. A 16-bit serial-output analog-to-digital converter (ADC) ADS7809 from Texas Instruments Incorporated is used

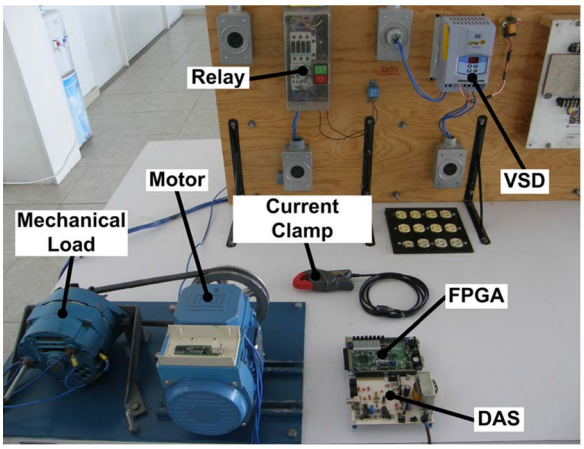

Fig. 8. Experiment setup for acquiring voltage and electric current supply signals to an induction motor for time-frequency analysis.

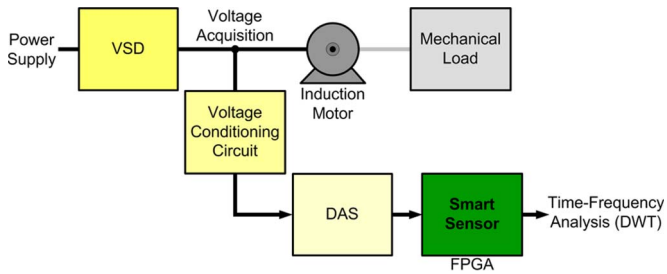

Fig. 9. Methodology to perform time-frequency analysis utilizing the proposed smart sensor on the voltage signal supplied to an induction motor through a VSD.

in the DAS. The monitored voltage signal is conditioned and then acquired utilizing the DAS. The instrumentation system uses a sampling frequency $f_0 = 750$ Hz for rotational speed at 30 and 45 Hz and $f_0 = 1.5$ kHz for rotational speed at 60 Hz, obtaining 4096 samples on each case, acquiring up to the tenth harmonic and beyond. Finally, the discrete voltage signal is time-frequency analyzed by the proposed SoC-based smart sensor implemented into the FPGA. Fig. 9 depicts the applied methodology.

B. Experiment Setup for Electric Current Signal Analysis

The startup transient current signal of an induction motor can be used for finding time-dependent harmonics related to some fault. The induction motor described in Section IV-A, but now with broken bars, is used to test the performance of the proposed SoC-based smart sensor on carrying out a time-frequency analysis of electric current supply signals, as depicted in Fig. 8. The motor receives a power supply of 220-V ac at 60 Hz. The applied mechanical load is that of an ordinary alternator, which represents a quarter of load for the motor. One phase of the current signal is acquired using an ac current clamp model i200s from Fluke. The motor start is controlled by a relay in order to synchronize the data acquisition with the motor switch on. The monitored electric current is conditioned and then acquired, utilizing the DAS described in Section IV-A. The instrumentation system utilizes a sampling frequency $f_0 =$ 3 kHz, obtaining 4096 samples of the induction motor startup

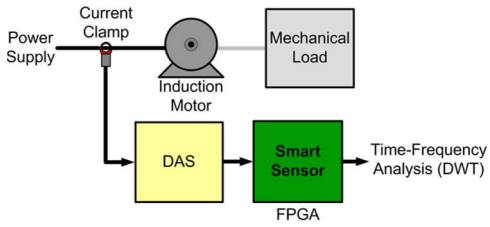

Fig. 10. Methodology to carry out time-frequency analysis of the electric current signal supplied to an induction motor utilizing the proposed smart sensor.

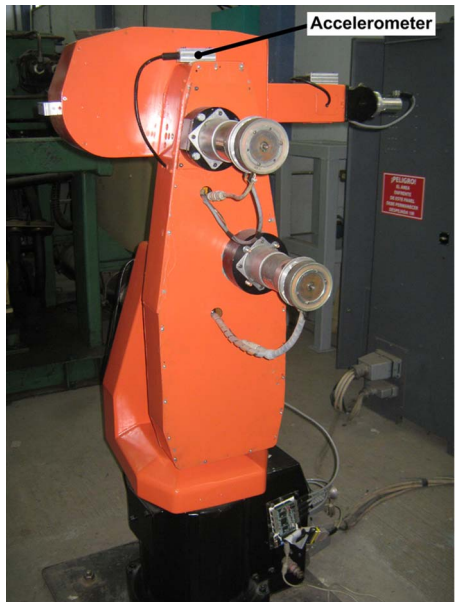

Fig. 11. Experiment setup for acquiring vibration signals on the second effector of an industrial robot arm for time-frequency analysis.

transient. Finally, the discrete current signal is time-frequency analyzed utilizing the proposed SoC-based smart sensor implemented into the FPGA, as shown in Fig. 10.

C. Experiment Setup for Vibration Signal Analysis

Fig. 11 shows the experiment setup and location of the vibration sensor used during the time-frequency analysis of transient signals on industrial robot links. The experiment consists of a single-axis movement of the second effector arm using a motion controller to apply a seventh-order polynomial motion profile during 32 s. Related vibration signals are extracted to carry out wavelet packet analysis through the proposed SoC-based smart sensor.

The experiment involves the instrumentation of a single axis for a 6-degree of freedom Cloos-Romat 56 modular robot. A MEMS-based 3-axial accelerometer model LIS3L02AS4 is used for this purpose. Because of the arm slow movement, transient vibrations are low frequency; therefore, a low sampling rate $f_0 = 50$ Hz is required. A 12-bit four-channel serial-output ADC model ADS7841 is used in the DAS. The discrete 3-axis vibration signals are forwarded to the FPGA, which contains the hardware implementation of the proposed smart sensor for time-frequency analysis. Fig. 12 shows the applied methodology. The vibration signals from the second effector arm are

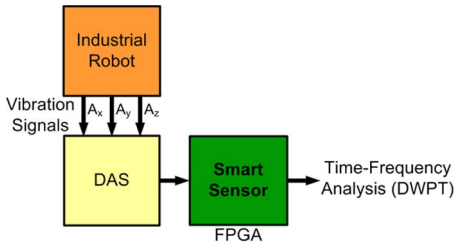

Fig. 12. Methodology to carry out time-frequency analysis of vibration signals on the second effector of a robot arm utilizing the proposed smart sensor.

TABLE I
CRITICAL CASE HARDWARE IMPLEMENTATION FIGURES FOR THE PROPOSED SMART SENSOR

	Xilinx Spartan-3		Altera Cyclone-II	
Resource	Used	Available	Used	Available
Programmable Logic	5,086	7,680	8,050	33,216
Block RAM	24	24	402,432	483,840
18×18MULT	7	24	14	70
Max. Op. Frequency	**54.44 MHz**		**51.48 MHz**	

conditioned and analog-to-digital converted in the DAS. The resulting digital information is time-frequency analyzed by the smart sensor in the FPGA.

D. Smart Sensor Hardware Implementation Results

Table I summarizes the hardware implementation figures of the proposed smart sensor for time-frequency analysis of a signal in an FPGA from two different vendors, i.e., Spartan-3 XC3S1000 from Xilinx and Cyclone II EP2C35F672C6 from Altera. This table presents the number of utilized resources against the number of available resources, as well as the corresponding maximum operation frequency for each device. Each reported figure represents the critical case of implementation.

The proposed SoC-based smart sensor takes 122 880 clock cycles for time-frequency decomposition, which is equivalent to 2.257 ms in a Xilinx Spartan-3 device and 2.386 ms in an Altera Cyclone II device running at their corresponding maximum operational frequency. Both hardware implementations outperform by one order of magnitude the software implementation counterpart, which takes 11.373 ms to estimate the signal decomposition in a 2.8-GHz Intel Pentium Dual Core processor. Fig. 13 shows the FPGA implementation of the proposed smart sensor in an Altera DE2 board. The resulting time-frequency analysis is shown on a VGA screen and/or an LCD.

E. Voltage Signal Analysis Results

VSD operation is based on pulsewidth modulation commutations. They generate many harmonics on the output signal compromising the detectability of time-dependent frequencies in an induction motor fed by the VSD [25]. The voltage supply signal fed to the induction motor through the VSD at rotational speeds of 30, 45, and 60 Hz is analyzed, utilizing DWT. Fig. 14(a)–(f) shows 2-D and 3-D views of time-frequency analyses obtained by the proposed smart sensor. Each figure shows the normalized voltage supply signal V fed to the induction motor, reconstruction of level-5 approximation

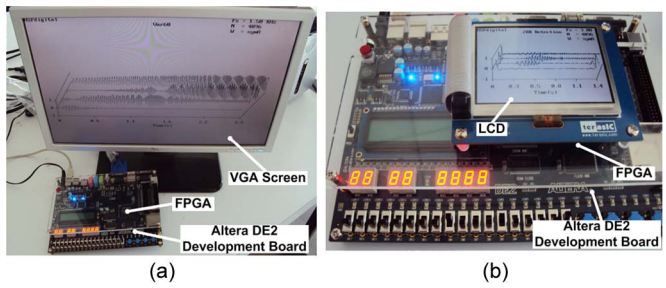

Fig. 13. Implementation of the proposed smart sensor in a DE2 Development Board with time-frequency analysis results graphically shown on (a) VGA screen and (b) LCD.

AC_5, level-5 decomposition DC_5, and level-4 decomposition DC_4. They correspond to the frequency bands [0–11.71 Hz], [11.71–23.43 Hz], and [23.43–46.87 Hz], respectively, for 30- and 45-Hz rotational speeds, and to frequency bands [0–23.43 Hz], [23.43–46.87 Hz], and [46.87–93.75 Hz], respectively, for 60-Hz rotational speed. Obtained results (see Fig. 14) show the VSD effects on the supply voltage to the induction motor. The voltage signal starts at 0 Hz and increases up to the desired rotational frequency, creating a chirp effect. The signal distributes among different frequency bands as its nominal frequency is increased in time by the VSD.

F. Electric Current Signal Analysis Results

During the startup transient, the motor accelerates, following a succession of stationary regimes with increasing speeds. Under such condition, the broken-rotor-bar frequency continuously changes. It starts being equal to the nominal supply frequency when the motor is switched on. As the rotor accelerates, the broken-bar frequency decreases to 0 Hz during the first half of the startup transient. Through the second half of the startup transient, the broken-bar frequency increases, nearly reaching the nominal supply frequency. During the steady-state regime, it keeps a constant value close to the nominal supply frequency [14], [26]. Fig. 15(a)–(d) shows 2-D and 3-D views of time-frequency analysis provided by the proposed smart sensor. The electric current supply signals to a healthy induction motor and an induction motor with broken rotor bars are analyzed and compared, utilizing DWT. Fig. 15 shows the normalized current supply signal I fed to the induction motor, reconstruction of level-7 approximation AC_7, level-7 decomposition DC_7, and level-6 decomposition DC_6. They correspond to the frequency bands [0–11.71 Hz], [11.71–23.43 Hz], and [23.43–46.87 Hz], respectively. Comparing the obtained time-frequency analyses, the time evolution effects of the broken-rotor-bar frequency on the electric current supply can be easily noticed.

G. Vibration Signal Analysis Results

The vibration signals on each axis of the robot arm are related to the motion profile, and they are time dependant. On each axis, vibrations rapidly increase at the beginning of the arm movement. They almost disappear as the arm reaches a steady and continuous displacement. Suddenly, vibrations increase and decrease as the arm arrives to its final position [27]. The

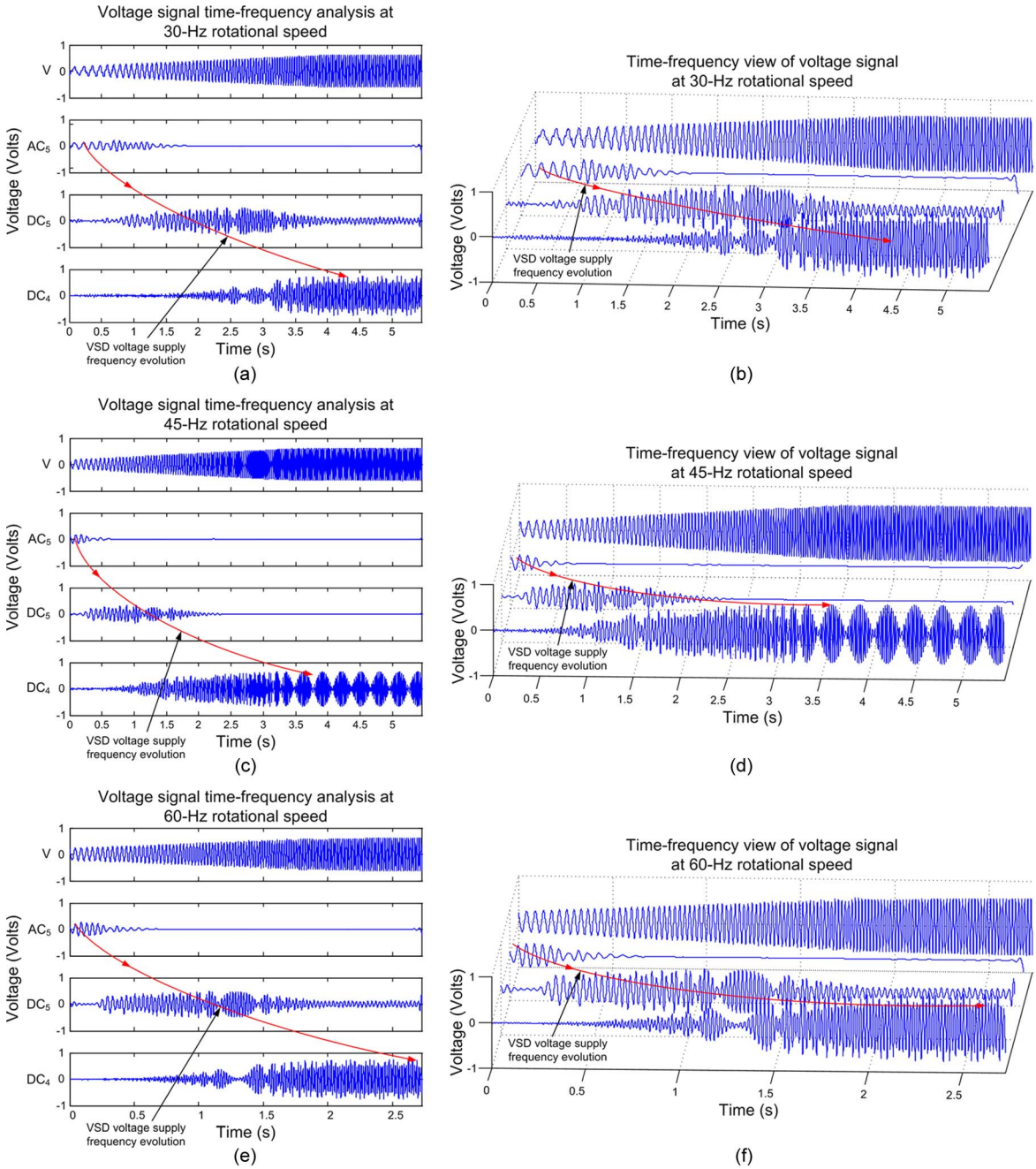

Fig. 14. Time-frequency analysis obtained by the proposed smart sensor from the voltage signal fed to the induction motor through the VSD. (a) 2-D view and (b) 3-D view at 30-Hz rotational speed. (c) 2-D view and (d) 3-D view at 45-Hz rotational speed. (e) 2-D view and (f) 3-D view at 60-Hz rotational speed.

X-, Y-, and Z-axis vibration signals from the second effector arm are analyzed, utilizing DWPT. Fig. 16(a)–(f) shows 2-D and 3-D views of time-frequency analysis results provided by the proposed smart sensor. Each figure shows the normalized vibration signal (A_x, A_y, and A_z) on the robot arm and reconstruction of nodes $S_{3,7}$, $S_{3,6}$, and $S_{3,2}$, which correspond to frequency bands [21.875–25 Hz], [18.75–21.875 Hz], and [3.125–6.25 Hz], respectively. Obtained time-frequency analysis (see Fig. 16) shows the vibration frequency evolution on each axis at the beginning and end of the robot arm movement. It also shows how high- and low-frequency components distribute among different frequency bands in time, appearing and disappearing as the robot arm moves.

H. Discussion

Obtained results demonstrate that the proposed smart sensor can be used for time-frequency analysis of diverse signals such as voltage, electric current, vibrations, and many more, acquired with different primary sensors. Smart sensors in discussed literature can be considered application specific since they just process particular signals acquired by a specific primary sensor. The proposed smart sensor is based on a reconfigurable SoC design that allows the implementation of two different time-frequency analysis techniques, i.e., DWT and DWPT. Due to its reconfigurability, the user can define several parameters for the applied technique during implementation so that the time-frequency evolution effects on the analyzed

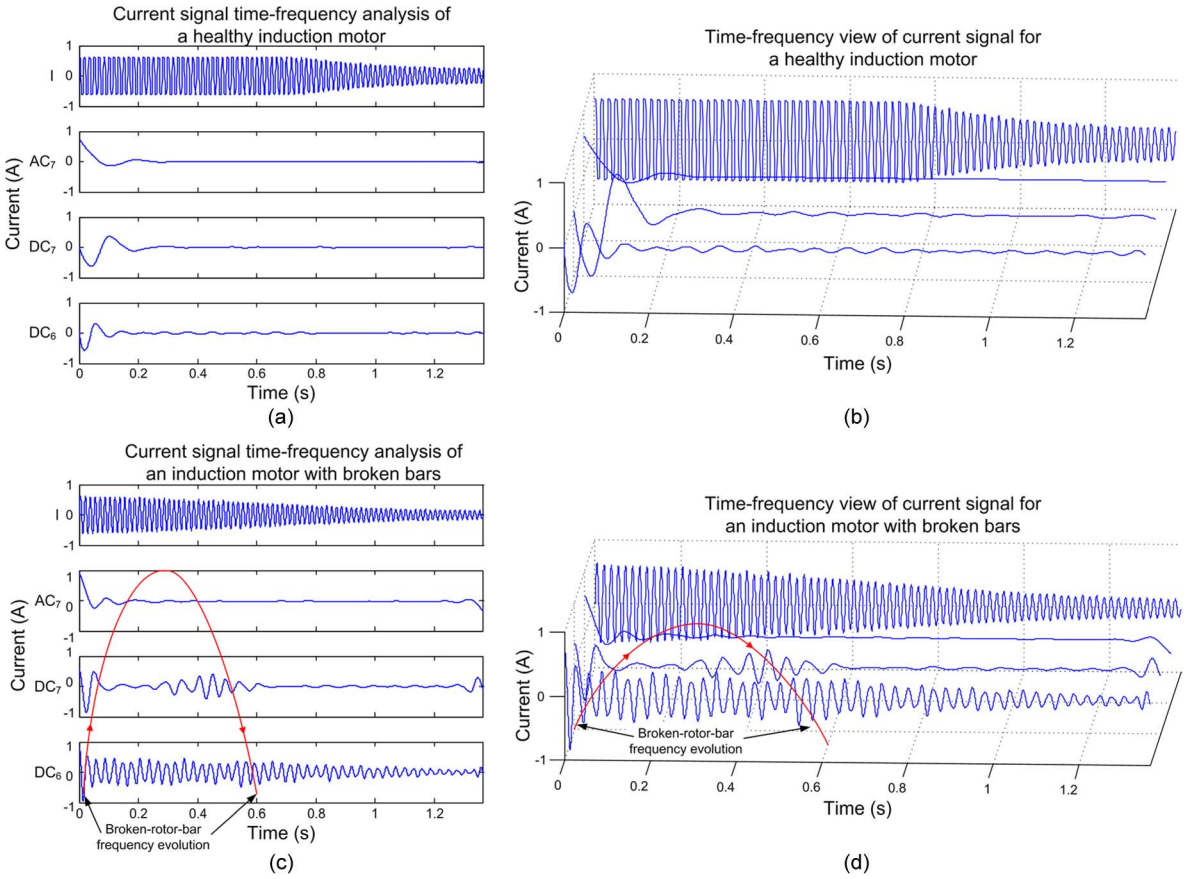

Fig. 15. Time-frequency analysis obtained by the proposed smart sensor from the electric current supply. (a) 2-D view and (b) 3-D view from the healthy induction motor. (c) 2-D view and (d) 3-D view from the induction motor with broken rotor bars.

signal can be observed to a greater extent. This overcomes previously proposed techniques that just implement wavelet decomposition, or decomposition and reconstruction, for specific levels or nodes with a particular wavelet mother function on a fixed-length acquired signal. The versatility of the proposed smart sensor makes it portable and easy to interconnect with different monitoring systems based on distinct primary sensors utilizing different interfaces. One significant characteristic of the proposed smart sensor is its way of presenting results. It can work as a standalone system by providing graphical results on a VGA screen and/or an LCD in a 2-D or 3-D user-selected visualization. Results can be also streamed out to a PC for additional processing, utilizing different interfaces. Furthermore, different from any other FPGA-based embedded system solution for time-frequency analysis, the selectable 2-D and 3-D visualizations allow examining the signal frequency evolution in time from different perspectives to extract relevant time-dependent information. The usefulness of the proposed smart sensor for system monitoring through time-frequency analysis is validated by obtained results from the treated study cases: detection of time-dependent harmonics on the voltage signal provided by a VSD (see Fig. 14), identification of frequency components related to broken rotor bars in the electric current supply to an induction motor (see Fig. 15), and observation of the frequency evolution in vibration signals from each axis during the movement of a robot arm (see Fig. 16).

V. Conclusion

This paper has presented a low-cost SoC-based smart sensor with a reconfigurable architecture for time-frequency analysis of different signals acquired by distinct primary sensors. The proposed smart sensor implementation is based on a low-cost FPGA device that adds characteristics of real-time processing, portability, and versatility, making it a helpful SoC solution for many applications. The proposed smart sensor features allow connecting it to other monitoring systems or a PC through different interfaces without additional instrumentation or equipment. Its reconfigurability permits modification or redefinition of the implemented signal processing technique for time-frequency analysis (DWT or DWPT), with different parameters (e.g., mother wavelet function and decomposition level) without changing the hardware itself. Different from many monitoring systems for time-frequency analysis discussed in reviewed literature, the proposed smart sensor provides online results in real time through a VGA screen and/or an LCD in a 2-D or 3-D view, which can be selected by the user. Obtained results demonstrate the effectiveness of the proposed smart sensor on showing online and in real-time frequency evolution effects in distinct time-varying signals from three different cases of study: detection of time-dependent harmonics on the voltage signal provided by a VSD, identification of frequency components related to broken rotor bars in the electric current supply to an induction motor, and observation of the frequency evolution in vibration signals from each axis

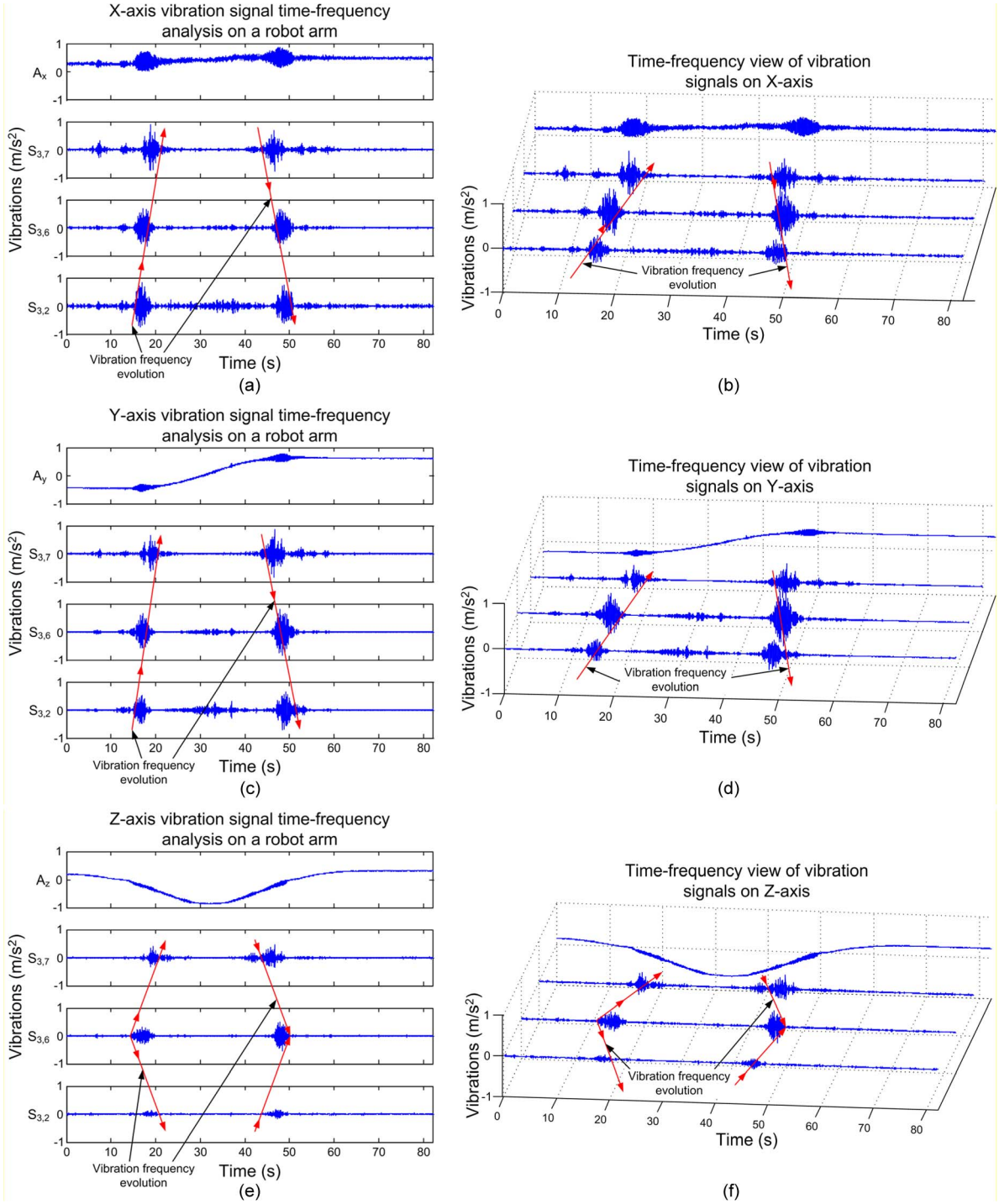

Fig. 16. Results of the proposed smart sensor during time-frequency analysis of vibration signals on the robot arm second effector. (a) 2-D view and (b) 3-D view of X-axis vibrations. (c) 2-D view and (d) 3-D view of Y-axis vibrations. (e) 2-D view and (f) 3-D view of Z-axis vibrations.

during the movement of a robot arm. Other signals can be monitored utilizing the proposed smart sensor by connecting the corresponding primary sensor and accordingly configuring the DAS during the smart sensor implementation. This way, the proposed smart sensor outperforms commercially available equipment and previous solutions, which are usually designed for processing a particular signal acquired by a specific primary sensor.

REFERENCES

[1] R. Frank, *Understanding Smart Sensors*. Norwood, MA: Artech House, 2000.

[2] K. Watanabe, T. Ishigaki, and T. Higuchi, "A multivariable detection device based on a capacitive microphone and its application to security," *IEEE Trans. Instrum. Meas.*, vol. 59, no. 7, pp. 1955–1963, Jul. 2010.

[3] M. Cole, J. A. Covington, and J. W. Gardner, "Combined electronic nose and tongue for flavor sensing system," *Sens. Actuators B, Chem.*, vol. 156, no. 2, pp. 832–839, Aug. 2011.

[4] S. Saponara, E. Petri, L. Fanucci, and P. Terreni, "Sensor modelling, low-complexity fusion algorithms, and mixed-signal IC prototyping for gas measures in low-emission vehicles," *IEEE Trans. Instrum. Meas.*, vol. 60, no. 2, pp. 372–384, Feb. 2011.
[5] L. Huimin, L. Weilin, L. Min, A. Monti, and F. Ponci, "Design of smart MVDC power grid protection," *IEEE Trans. Instrum. Meas.*, vol. 60, no. 9, pp. 3035–3046, Sep. 2011.
[6] D. Granados-Lieberman, R. J. Romero-Troncoso, E. Cabal-Yepez, R. A. Osornio-Rios, and L. A. Franco-Gasca, "A real-time smart sensor for high-resolution frequency estimation in power systems," *Sensors (Basel)*, vol. 9, no. 9, pp. 7412–7429, Sep. 2009.
[7] J.-D. Son, G. Niu, B.-S. Yang, D.-H. Hwang, and D.-S. Kang, "Development of smart sensors system for machine fault diagnosis," *Expert Syst. Appl.*, vol. 39, no. 9, pp. 11 981–11 991, Nov. 2009.
[8] A. Depari, A. Flammini, D. Marioli, and A. Taroni, "USB sensor network for industrial applications," *IEEE Trans. Instrum. Meas.*, vol. 57, no. 7, pp. 1344–1349, Jul. 2008.
[9] S. V. Moreno-Tapia, L. A. Vera-Salas, R. A. Osornio-Rios, A. Dominguez-Gonzalez, I. Stiharu, and R. J. Romero-Troncoso, "A field programmable gate array-based reconfigurable smart-sensor network for wireless monitoring of new generation computer numerically controlled machines," *Sensors (Basel)*, vol. 10, no. 8, pp. 7263–7286, Aug. 2010.
[10] J. A. Gomez-Pulido, "From systems to networks on chip: A promising research area in the hardware/software co-design," *J. Syst. Architect.*, vol. 56, no. 7, pp. 221–222, Jul. 2010.
[11] L. M. Morales-Velazquez, R. J. Romero-Troncoso, R. A. Osornio-Rios, G. Herrera-Ruiz, and E. Cabal-Yepez, "Open-architecture system based on a reconfigurable hardware–software multi-agent platform for CNC machines," *J. Syst. Architect.*, vol. 56, no. 9, pp. 407–418, Sep. 2010.
[12] H. Yuan, J. Gao, H. Z. Guo, and C. Lu, "An efficient method to process the quantized acoustoelectric current: Wavelet transform," *IEEE Trans. Instrum. Meas.*, vol. 60, no. 3, pp. 696–702, Mar. 2011.
[13] J. P. Amezquita-Sanchez, E. Cabal-Yepez, R. J. Romero-Troncoso, R. A. Osornio-Rios, and A. Garcia-Perez, "Determination of system frequencies in mechanical systems during shutdown transient," *J. Sci. Ind. Res. India*, vol. 69, pp. 415–421, Jun. 2010.
[14] A. Ordaz-Moreno, R. J. Romero-Troncoso, J. A. Vite-Frias, J. R. Rivera-Guillen, and A. Garcia-Perez, "Automatic online diagnosis algorithm for broken-bar detection on induction motors based on discrete wavelet transform for FPGA implementation," *IEEE Trans. Ind. Electron.*, vol. 55, no. 5, pp. 2193–2202, May 2008.
[15] D. G. Ece and M. Basaran, "Condition monitoring of speed controlled induction motors using wavelet packets and discriminant analysis," *Expert Syst. Appl.*, vol. 38, no. 7, pp. 8079–8086, Jul. 2011.
[16] E. C. C. Lau and H. W. Ngan, "Detection of motor bearing outer raceway defect by wavelet packet transformed motor current signature analysis," *IEEE Trans. Instrum. Meas.*, vol. 59, no. 10, pp. 2683–2690, Oct. 2010.
[17] N. Y. Steiner, D. Hissel, P. Mocoteguy, and D. Candusso, "Non intrusive diagnosis of polymer electrolyte fuel cells by wavelet packet transform," *Int. J. Hydrogen Energy*, vol. 36, no. 1, pp. 740–746, Jan. 2011.
[18] G. A. Kaiser, *Friendly Guide to Wavelets*. Boston, MA: Birkhäuser, 1994.
[19] S. Mallat, *A Wavelet Tour of Signal Processing, The Sparse Way*, 3rd ed. Burlington, MA: Elsevier, 2009.
[20] R. R. Coifman, Y. Meyer, and M. V. Wickerhauser, "Wavelet analysis and signal processing," in *Wavelets and Their Applications*. Boston, MA: Jones & Bartlett, 1992, pp. 153–178.
[21] L. Fannuci, S. Saponara, and A. Morello, "Power optimization of an 8051-compliant IP microcontroller," in *IEICE Trans. Electron.*, Apr. 2005, vol. E88-C, no. 4, pp. 597–600.
[22] B. Donchev, "Design of low power automotive interface," in *Proc. 27th Int. Spring Semin. Electron. Technol.: Meeting Challenges Electron. Technol. Progr.*, Bankya, Bulgaria, 2004, pp. 377–382.
[23] J. E. O. Rages and E. J. P. Santos, "A VHDL CAN module for smart sensors," in *Proc. 4th Southern Conf. Program. Logic*, San Carlos de Bariloche, Argentina, 2008, pp. 179–182.
[24] F. Baronti, E. Petri, S. Saponara, L. Fannuci, R. Roncella, R. Saletti, P. D'Abramo, and R. Serventi, "Design and verification of hardware building blocks for high-speed and fault-tolerant in-vehicle networks," *IEEE Trans. Ind. Electron.*, vol. 58, pp. 792–801, Mar. 2011.
[25] J. R. Millan-Almaraz, R. J. Romero-Troncoso, R. A. Osornio-Rios, and A. Garcia-Perez, "Wavelet-based methodology for broken bar detection in induction motors with variable-speed drive," *Elect. Power Compon. Syst.*, vol. 39, no. 3, pp. 271–287, Jan. 2011.
[26] M. Riera-Guasp, J. A. Antonino-Daviu, M. Pineda-Sanchez, R. Puche-Panadero, and J. Perez-Cruz, "A general approach for the transient detection of slip-dependent faults components based on the discrete wavelet transform," *IEEE Trans. Ind. Electron.*, vol. 55, no. 12, pp. 4167–4180, Dec. 2008.
[27] C. Rodriguez-Donate, L. M. Morales-Velazquez, R. A. Osornio-Rios, G. Herrera-Ruiz, and R. J. Romero-Troncoso, "FPGA-based fused smart sensor for dynamic and vibration parameter extraction in industrial robot links," *Sensors (Basel)*, vol. 10, no. 4, pp. 4114–4129, Apr. 2010.

Rene J. Romero-Troncoso (M'07) received the B.E. and M.E. degrees in electronics from the University of Guanajuato, Salamanca, Mexico, and the Ph.D. degree in mechatronics from the Autonomous University of Queretaro, Queretaro, Mexico.

He is currently a Head Professor with the University of Guanajuato and an Invited Researcher with the Autonomous University of Queretaro. He is a National Researcher with the Consejo Nacional de Ciencia y Tecnologia. He has been an Adviser of more than 150 theses, an author of two books on digital systems (in Spanish), and a coauthor of more than 40 technical papers in international journals and conferences. His fields of interest include hardware signal processing and mechatronics.

Dr. Romero-Troncoso was the recipient of the "2004 ADIAT National Award on Innovation" for his works in applied mechatronics and the "2005 IEEE ReConFig'05" Award for his works in digital systems.

Marcos Pena-Anaya received the B.Eng. degree (with Honors) from the Instituto Tecnológico de Mazatlán, Mazatlan, Mexico, and the Master's degree (with Honors) from the Universidad de Guanajuato, Salamanca, Mexico, where he did research work at the HSPdigital Group.

His research interests include hardware signal processing and embedded systems on a field-programmable gate array for applications on mechatronics.

Eduardo Cabal-Yepez (M'09) received the B.Eng. and M.Eng. degrees from the University of Guanajuato, Salamanca, Mexico, and the D.Phil. degree from the University of Sussex, Brighton, U.K.

He is currently a Titular Professor with the Division of Engineering, University of Guanajuato doing research work at the HSPdigital Group, which is focused on hardware signal processing on field-programmable gate arrays for applications in mechatronics. He is a National Researcher with the Consejo Nacional de Ciencia y Tecnologia.

Arturo Garcia-Perez (M'10) received the B.E. and M.E. degrees in electronics from the University of Guanajuato, Salamanca, Mexico, and the Ph.D. degree in electrical engineering from the University of Texas at Dallas, Richardson, in 1992, 1994, and 2005, respectively.

He is currently a Titular Professor with the Department of Electronic Engineering, University of Guanajuato. He has been an Adviser of over 40 thesis. His fields of interest include digital signal processing for applications in mechatronics.

Roque A. Osornio-Rios (M'10) received the B.E. degree from the Instituto Tecnológico de Querétaro, Queretaro, Mexico, and the M.E. and Ph.D. degrees from the Autonomous University of Queretaro, Queretaro.

He is a National Researcher with the Consejo Nacional de Ciencia y Tecnologia. He is currently a Head Professor with the Autonomous University of Queretaro, San Juan del Rio, Mexico. He has been an Adviser of more than 20 theses and the coauthor of more than 23 technical papers in international journals and conferences. His fields of interest include hardware signal processing and mechatronics.

Dr. Osornio-Rios was the recipient of the "2004 ADIAT National Award on Innovation" for his works in applied mechatronics.